EXPERIMENTAL STUDY OF FREE CONVECTION WITH POROUS BLOWING AND SUCTION ON A VERTICAL SURFACE

P. M. Brdlik and V. A. Mochalov

Inzhenerno-Fizicheskii Zhurnal, Vol. 10, No. 1, pp. 3–10, 1966

UDC 536.25

The paper presents the results of an experimental study of the heat transfer and the temperature field in a free-convection boundary layer on a vertical surface with uniform porous blowing and suction and T_w = const. The method of measurement is described and the experimental data are compared with the theoretical results obtained by the authors in an earlier work. The experiments were carried out on a Zender-Mach interferometer. The theoretical and experimental results are found to be in good agreement. Critical values of the parameters are found, which determine the beginning of the transient and developed turbulent regions as a function of the rate of blowing or suction.

Experimental setup. An experimental setup, shown in Fig. 1, was constructed in order to check the theoretical results obtained by the authors in an earlier work [5]. The experiments were performed on porous copper plates with a coefficient of porosity of approximately 0.5. Five plates were used, with a working area of 200 × 300 mm and about 10 mm thickness. The plates were mounted in profile slots in textolite housings flush with the surface of the housings, so that the total working area was 1000 mm high by 300 mm wide. Each housing was hermetically sealed and had a separate heating and blowing system. The air was blown in and sucked out by fans. Air flow was measured by means of RS-5a and RS-3a rotameters, calibrated with a non-standard orifice. The velocity of the air being blown in or out could be varied in a wide range. The maximum error in air flow measurements was about 4%. The air blown in was filtered.

The plates were heated by means of radiators mounted in the textolite housings, so that the change-over from blowing to suction did not require any modifications of the set-up.

The radiators consisted of a double row of infrared encandescent bulbs with mirror coating. Each bulb also had its own reflector of aluminum foil. The inside of each housing was covered with foil. This arrangement heated the porous copper plate to a uniform temperature, which could be adjusted by varying the voltage across the heating circuit. The uniformity of the temperature was checked by nine chromel-copel (a Cu–Ni alloy) thermocouples embedded in the plate. During the experiments, the surface temperature of the porous plate and the power supplied to the radiators were regulated. The temperature of the blown and sucked air was measured by three chromel-copel thermocouples in the immediate vicinity of the plate and at the inlet to the textolite housing. These thermocouples had radiation screens in the form of foil cylinders of 25 mm length.

The thermocouples which were embedded in the plate were used only for regulation, not for surface temperature measurement. Steady state, as indicated

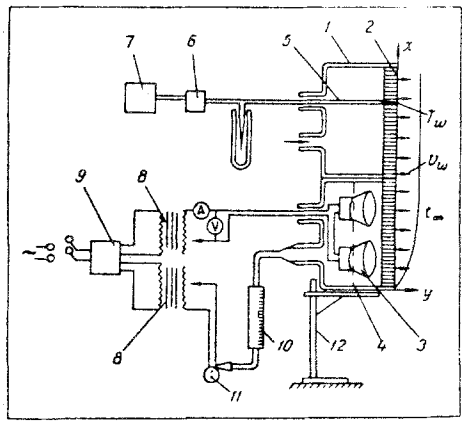

Fig. 1. Experimental set-up. 1) textolite housing; 2) porous copper plate; 3) radiators; 4) radiation screen; 5) thermocouples; 6) switch; 7) potentiometer; 8) regulating transformer; 9) stabilizer; 10) rotameter; 11) fan; 12) stand.

by these thermocouples, was reached in about 50 min in the case of low blowing (suction) and in about 30 min with maximum blowing (suction).

The temperature field in the boundary layer and the wall temperature were measured by means of a IZK-454 Zender-Mach interferometer with a field of 225 + 5 mm diameter.

The plate housings were mounted on a vertically-adjustable stand, so that any portion of the plate could be observed by the interferometer. The optical length of the model, i.e., the path of the light beam, was 300 mm. The monochromatic beam was obtained from a DRSh-250 mercury lamp with a monochromator. The photographs were taken with the interferometer adjusted both for infinite and finite fringe width. The processing of the interferograms and the calculation of the temperature field from the density field were in accordance with the method of [7].

As might be expected, blowing and suction had a marked effect on the free-convection boundary layer and temperature field (Fig. 2).

Compared with the case of an impermeable surface (Fig. 2c), suction makes the boundary layer thinner and the temperature profile fuller (Fig. 2a, b).

Blowing results in a swelling of the boundary layer and the appearance of an inflection point in the temperature profile (Fig. 2d). This effect is particularly

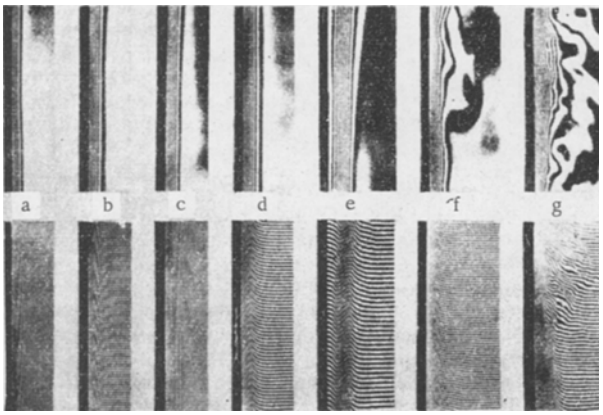

Fig. 2. Interferograms of the thermal boundary layer (upper row) and of the temperature field (bottom row) in free convection on a porous plate for various values of η : a) $\eta < -1.0$; b) $\eta = -0.5$; c) $\eta = 0.6$; e) $\eta > 1.0$; f) transition zone for $\eta = 0.4$; g) turbulent region for $\eta = 0.5$.

noticeable with values $\eta \gg 1.0$ (Fig. 2e), when the boundary layer is pushed away from the wall, and a sublayer with temperature equal to that of the wall appears underneath.

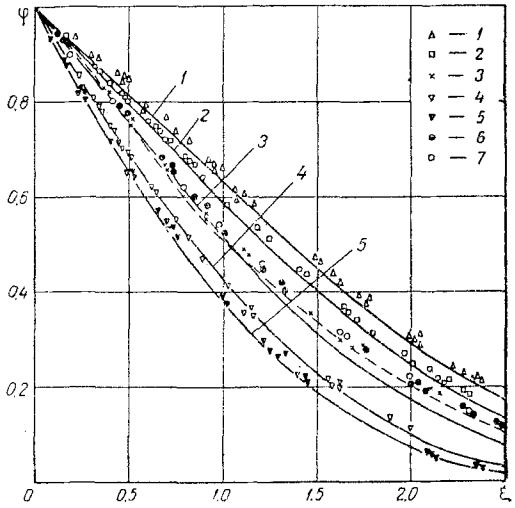

Fig. 3. Comparison of experimental and theoretical data on the temperature distribution in the boundary layer: continuous lines—according to equation (6); broken line—according to Pohlhausen; 1, 2, 3, 4, 5) experimental data obtained in the present work for $\eta = 0.6$, 0.4, 0, −0.4, and −0.6, respectively; 6) Soehengen's data [2]; 7) Malozemov's data [7].

The deformation of the temperature field in the boundary layer for low values of the blowing (suction) parameter can be seen in Fig. 3, which shows the temperature profiles in φ–ξ coordinates. The curves labeled 3 in the center of Fig. 3 represent the case of an impermeable plate ($\eta = 0$). The broken line represents Pohlhausen's exact solution [3], and the continuous curve represents the authors' solution [5] for $\eta = 0$. Fig. 3 also shows experimental data for $\eta = 0$ taken from [2, 7]. Curves 1, 2 represent blowing and curves 4, 5 represent suction. It is interesting to note that the temperature profile corresponding to $\eta = 0.6$ (Curve 1) has an inflection point. The theoretical temperature profiles are based on [5]. The experimental points are based on the interferograms taken by the authors. It can be seen from Fig. 3 that the approximate solution of [5] is in a quite satisfactory agreement with the experimental data.

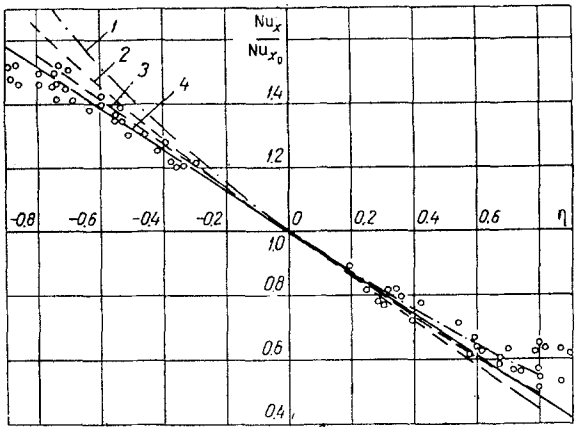

Fig. 4. Comparison of experimental and calculated values of the heat transfer coefficient in natural convection with blowing and suction: 1) according to [5]; 2) according to equation (10); 3) according to [1]; 4) according to equation (17).

The wall temperature calculated from the interferograms agreed with the thermocouple readings to within 0.2° C. The error associated with the evaluation of the interferograms is 0.1 fringe, which results in an error of about 3% in the calculation of the dimensionless temperature φ. We did not take into account the refraction of light beams due to the density gradient in the boundary layer near the wall, which could produce an error of 1%.

The local values of the heat transfer coefficient were calculated from the temperature fields obtained from the interferograms. These values are shown in Fig. 4 as a function of the dimensionless blowing (suction) parameter η. Fig. 4 also shows curves obtained from theoretical solutions. In order to demonstrate the effectiveness of blowing (suction) the values of the heat transfer coefficient are normalized with respect to the local values of the Nusselt number for an impermeable surface Nu_{x_0}.

Curve 1 in Fig. 4 was obtained by the authors in [5], taking the first two non-zero terms of the solution. Taking into account the subsequent terms, we obtain

$$x = \left(\frac{g\beta\theta_w}{\nu^2}\right)\cdot\delta^4\left[\frac{504\cdot 4!}{f^{(4)}(\delta=0,\ \mathrm{Pr})}\right]^{-1}\times$$

$$\times\left[1-\frac{\mathrm{Re}_\delta f^{(5)}(\delta=0,\ \mathrm{Pr})}{5f^{(4)}(\delta=0,\ \mathrm{Pr})}+\right.$$

$$\left.+\frac{\mathrm{Re}_\delta^2 f^{(6)}(\delta=0,\ \mathrm{Pr})}{30f^{(4)}(\delta=0,\ \mathrm{Pr})}-\frac{\mathrm{Re}_\delta^3 f^{(7)}(\delta=0,\ \mathrm{Pr})}{210f^{(4)}(\delta=0,\ \mathrm{Pr})}+\ldots\right], \quad (1)$$

where $\mathrm{Re}_\delta = v_\omega\delta/\nu$ and the values of $f^{(i)}(\delta = 0,\ \mathrm{Pr})$ are tabulated for various values of Pr.*

Inverting the series (1), we obtain

$$\frac{\delta}{x} = \mathrm{Gr}_x^{-1/4}\left[\frac{504\cdot 4!}{f^{(4)}(\delta=0,\ \mathrm{Pr})}\right]^{1/4}\times$$

$$\times\left\{1+\frac{f^{(5)}(\delta=0,\ \mathrm{Pr})\,\mathrm{Re}_x\,\mathrm{Gr}_x^{-1}}{[f^{(4)}(\delta=0,\ \mathrm{Pr})]^2}\left(\frac{x}{\delta}\right)^3\frac{504\cdot 4!}{5}+\right.$$

$$+\left[2\left(\frac{f^{(5)}(\delta=0,\ \mathrm{Pr})}{5f^{(4)}(\delta=0,\ \mathrm{Pr})}\right)^2-\frac{f^{(6)}(\delta=0,\ \mathrm{Pr})}{30f^{(4)}(\delta=0,\ \mathrm{Pr})}\right]\times$$

$$\left.\times\left[\frac{504\cdot 4!}{f^{(4)}(\delta=0,\ \mathrm{Pr})}\right]^2\mathrm{Re}_x^2\,\mathrm{Gr}_x^{-2}\left(\frac{x}{\delta}\right)^6+\ldots\right\}^{1/4}. \quad (2)$$

To find explicitly the values of the relative thickness of the boundary layer δ/x from (2), we must use the method of successive approximations. As a first approximation we take the value of δ/x for an impermeable surface,

$$\delta/x = \mathrm{Gr}_x^{-1/4}\left[\frac{504\cdot 4!}{f^{(4)}(\delta=0,\ \mathrm{Pr})}\right]^{1/4}, \quad (3)$$

and as a second approximation we take the value of δ/x obtained in [5] on the basis of the first two non-zero terms of the series, i.e.,

$$\frac{\delta}{x} = \mathrm{Gr}_x^{-1/4}\left[\frac{504\cdot 4!}{f^{(4)}(\delta=0,\ \mathrm{Pr})}\right]^{1/4}\times$$

$$\times\left[1-\frac{f^{(5)}(\delta=0,\ \mathrm{Pr})\,\eta}{20\cdot\sqrt[4]{4}\,f^{(4)}(\delta=0,\ \mathrm{Pr})}\right]^{-1}. \quad (4)$$

Substituting (3) and (4) into (2), and carrying out the necessary transformations, we obtain, for Pr = 0.72,

first approximation:

$$\delta/x = 5.42\,\mathrm{Gr}_x^{-1/4}(1+1.07\eta+1.4\eta^2+\ldots)^{1/4}, \quad (5)$$

second approximation:

$$\delta/x = 5.42\,\mathrm{Gr}_x^{-1/4}(1+1.07\eta-0.503\eta^2+\ldots)^{1/4}. \quad (6)$$

The local heat transfer coefficient is given by the relation

$$\alpha_x = -\lambda\,\mathrm{grad}\,\theta|_w/(T_w - T_\infty). \quad (7)$$

Knowing the value of the temperature gradient at the wall [5], we have

$$\mathrm{Nu}_{x_0} = (x/\delta)\cdot 12/(6+\mathrm{Re}_\delta\,\mathrm{Pr}). \quad (8)$$

Substituting (5) and (6) into (8), we obtain, for Pr = = 0.72,

first approximation:

$$\mathrm{Nu}_x/\mathrm{Nu}_{x_0} = (1-0.71\eta+0.083\eta^2-\ldots), \quad (9)$$

second approximation:

$$\mathrm{Nu}_x/\mathrm{Nu}_{x_0} = (1-0.71\eta+0.086\eta^2-\ldots). \quad (10)$$

Equation (10) gives curve 2 in Fig. 4.

For practical purposes one often needs to know the mean value of the heat transfer coefficient. Integrating (7) from 0 to x, we obtain

$$\bar{\alpha} = \frac{1}{x}\int_0^x \alpha_x\,dx \quad (11)$$

or

$$\bar{\alpha}/\bar{\alpha}_0 = (1-0.532\eta+0.051\eta^2-\ldots), \quad (12)$$

where $\bar{\alpha}_0$ is the mean heat transfer coefficient on a vertical impermeable surface, equal to $4\alpha_{x_0}$ [3].

The amount of blowing (suction) was expressed in terms of the parameter

$$\eta = \frac{v_\omega x}{\nu}\left(\frac{\mathrm{Gr}_x}{4}\right)^{-1/4}$$

($\eta > 0$ for blowing and $\eta < 0$ for suction), which did not exceed unity. The Grashof number was based on the mean temperature of the boundary layer $(T_\omega + T_\infty)/2$, and the Reynolds number $\mathrm{Re}_x = v_\omega x/\nu$ was based on the kinematic viscosity corresponding to wall temperature.

The experiments show that there exists a qualitative analogy between forced and free convection with blowing or suction. This analogy touches upon the effect of blowing (suction) on heat transfer and the formation of the boundary layer.

Let us attempt to express the heat flux to the wall q_w in our problem in terms of experimental results obtained for the case forced convection with suction or blowing.

*For details, see [5].

By a systematization of published experimental data on laminar boundary layers on permeable surfaces in forced convection there has been obtained the empirical relation [6]

$$\frac{q_w}{q_{w_0}} = 1 - 1.82\left(\frac{m_2}{m_1}\right)^{1/3}\frac{\rho_w v_w}{\rho_\infty u_\infty}\left(\frac{u_\infty x}{\nu}\right)^{1/2}. \quad (13)$$

Let us assume that in the layer adjacent to the wall the heat transfer conditions are the same in free and forced convection [8]. Then equation (13), with $m_1 = m_2$, becomes

$$\frac{q_w}{q_{w_0}} = 1 - 1.82\frac{v_w}{u_1}\left(\frac{u_1 x}{\nu}\right)^{1/2}, \quad (14)$$

where

$$u_1 = 5.17\nu\,(0.952 + \mathrm{Pr})^{-1/2}(g\beta\theta_w/\nu^2)^{1/2}x^{1/2}. \quad (15)$$

Substituting (15) into (14), we obtain

$$\frac{q_w}{q_{w_0}} = 1 - 0.80\frac{v_w x}{\nu}(\mathrm{Gr}_x)^{-1/4}(0.952 + \mathrm{Pr})^{1/4} \quad (16)$$

or, for Pr = 0.72,

$$q_w/q_{w_0} = 1 - 0.645\mathrm{Re}_x(\mathrm{Gr}_x/4)^{-1/4}. \quad (17)$$

Equation (17) is in good agreement with experimental results and with the solutions obtained in [1, 5]. This equation is represented by curve 4 in Fig. 4.

Transition from laminar to turbulent flow. Due to the low values of the velocities in the free-convection boundary layer, very low values of blowing or suction velocity suffice to cause significant changes in the thickness of the boundary layer, temperature profiles, and velocity profiles. The experiments show that the laminar boundary layer retains its basic structure for $|\eta| \leq 1.0$.

For $0 < \eta \leq 1.0$ the boundary layer becomes thicker, and the temperature profiles become less full (Fig. 2d). The thickening of the boundary layer has the result that long waves appear more often. The amplitude of these waves increases with increasing η, and the flow becomes less stable with respect to external perturbations and transverse oscillations. These effects affect the location of the transition zone—its beginning moves upstream, and the laminar region becomes shorter,

For $-1.0 \leq \eta < 0$ the stability of the boundary layer with respect to external perturbations increases, its thickness decreases, and the temperature profiles move closer to the surface and become fuller (Fig. 2b). This has the effect that the location of the beginning of the transition zone and the beginning of the turbulent boundary layer move downstream.

Typical pictures of transition zone and developed turbulent flow are shown in Fig. 2f, g.

The location of the beginning of the transition zone was determined by the appearance of irregular perturbations, which, as can be seen in Fig. 2f, appear at a definite point of the surface and, consequently, at a definite value of the Brashof number. The Grashof number is the governing parameter in free convection, analogous to the Reynolds number in forced convection. The beginning of the fully-developed turbulent flow was determined by the appearance of eddies, which can be seen in Fig. 2f.

In the experiments we found the values η_1 and η_2 for which the beginning of the transition zone or the beginning of developed turbulent flow appeared at a given value of the Grashof number. The results of the interferograms were plotted in the form of Nu_X vs. Gr_X in logarithmic coordinates for various values of the parameter η. This made it possible to determine the location of the transition zone as a function of blowing (suction).

The location of the beginning of the transition zone can be represented by empirical formula

$$\mathrm{Gr}_1 = \mathrm{Gr}_{1_0}\left[1 - 0.3\frac{v_w x}{\nu}\left(\frac{\mathrm{Gr}_1}{4}\right)^{-1/4}\right], \quad (18)$$

and the beginning of the devloped turbulent flow can be represented by

$$\mathrm{Gr}_2 = \mathrm{Gr}_{2_0}\left[1 - 0.2\frac{v_w x}{\nu}\left(\frac{\mathrm{Gr}_2}{4}\right)^{-1/4}\right]. \quad (19)$$

In (18) and (19) the values Gr_{10} and Gr_{20} are those for an impermeable surface, in the case of air equal to 10^7 and 2×10^9 [4]. The formulas (18) and (19) were obtained with blowing (suction) extending over the whole transition zone and $|\eta| \leq 1.0$.

Properties of the boundary layer for large values of blowing (suction). It is interesting to consider the results of experiments with $|\eta| > 1.0$. For $n > 1.0$ there appears a film of air on the surface and the boundary layer "slips" on this film (Fig. 2e). This air film has finite thickness and constant temperature, equal to T_W. For $\mathrm{Gr}_X < 10^6$ the boundary layer, which is pushed away from the wall, retains its laminar structure and no mixing or irregular perturbations occur in it, irrespective of the value of the blowing parameter.

For $\eta < -1.0$ the thickness of the boundary layer sharply decreases and the temperature of the wall can approach, with constant heat load, the temperature of the surrounding gas.

These properties of the boundary layer for large values of blowing (suction) have the effect that the experimental in Fig. 4 which correspond to $|\eta|$ close to unity have a large scatter.

NOTATION

v_W—blowing or suction velocity; T—temperature; $\xi = y/x(\mathrm{Gr}_X/4)^{1/4}$—Pohlhausen's dimensionless coordinate; $\eta = v_\omega x/\nu(\mathrm{Gr}_X/4)^{-1/4}$—blowing or suction

parameter; $Re_\delta = v_\omega \delta/\nu$—Reynolds number, based on the blowing (suction) velocity and on the boundary layer thickness; $\varphi = (T - T_\infty)/(T_\omega - T_\infty)$—dimensionless temperature of the boundary layer; $Re_x = v_\omega x/\nu$—Reynolds number, based on the blowing (suction) velocity and the coordinate x; Gr_1 and Gr_2—Grashof numbers corresponding to the beginning of the transition zone and the beginning of developed turbulent flow; m_1 and m_2—molecular weights of main-stream and blown gas, respectively; q_{w_0}—heat flux on impermeable surface; u_1—a function, with the dimensions of velocity, given in [3].

REFERENCES

1. E. M. Sparrow and R. D. Cess, Trans. ASME, Series C, no. 3, 1961.

2. E. E. Soehengen, Actes IX Congr. Bruxells. Univ. Bruxells, 1957.

3. E. R. G. Eckert and R. M. Drake Jr., Heat and Mass Transfer [Russian translation], Gosenergoizdat, 1961.

4. O. A. Saunders, Roy. Soc. Proc., A, 172, 1939.

5. P. M. Brdlik and V. A. Mochalov, IFZh [Journal of Engineering Physics], 8, no. 2, 1965.

6. J. F. Gross and H. P. Hartnett, Jet Propulsion, 28, no. 10, 1958.

7. V. V. Malozemov and I. A. Turchin, IFZh [Journal of Engineering Physics], 8, no. 8, 1965.

8. E. R. G. Eckert and W. Fh. Jackson, NACA, Report 1015, 1951.

28 September 1965

Institute of Building Physics, Moscow